Figure S1

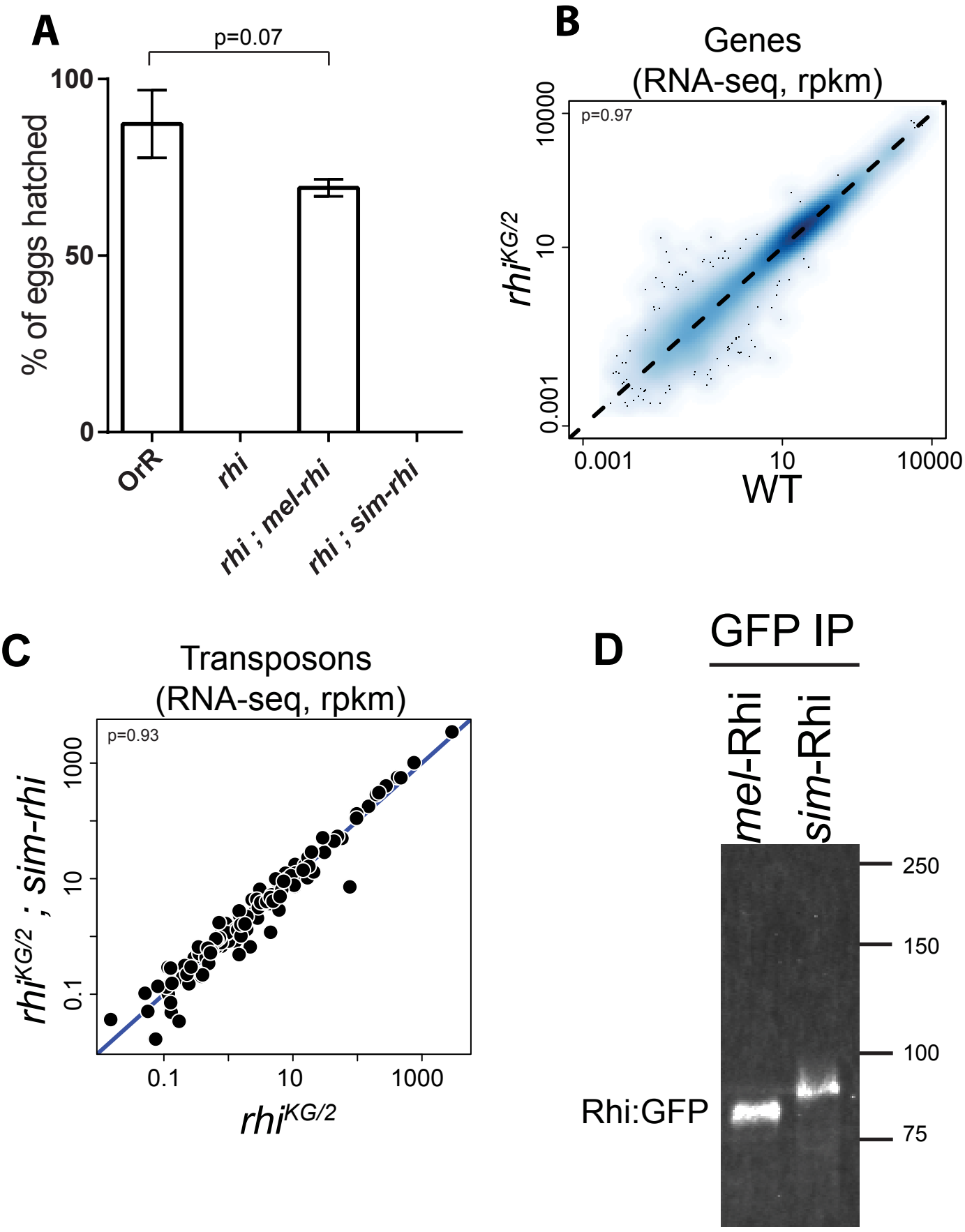
A
p=0.07
100
50
0
% of eggs hatched
OrR
rhi
rhi ; mel-rhi
rhi ; sim-rhi
B
Genes
(RNA-seq, rpkm)
p=0.97
10000
10
0.001
rhiKG/2
0.001
10
10000
WT
C
Transposons
(RNA-seq, rpkm)
p=0.93
1000
10
0.1
rhiKG/2 ; sim-rhi
0.1
10
1000
rhiKG/2
D
GFP IP
mel-Rhi
sim-Rhi
250
150
100
75
Rhi:GFP

Figure S2

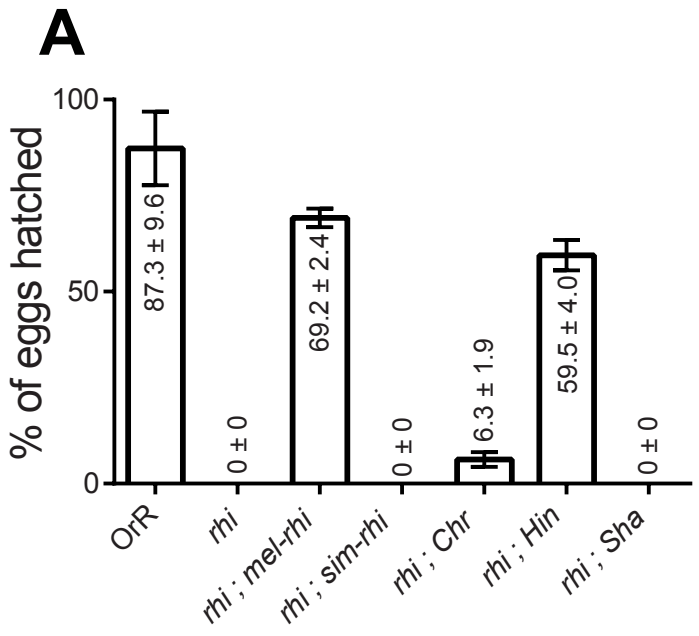
A
% of eggs hatched
100
50
0
87.3 ± 9.6
0 ± 0
69.2 ± 2.4
0 ± 0
6.3 ± 1.9
59.5 ± 4.0
0 ± 0
OrR
rhi
rhi ; mel-rhi
rhi ; sim-rhi
rhi ; Chr
rhi ; Hin
rhi ; Sha

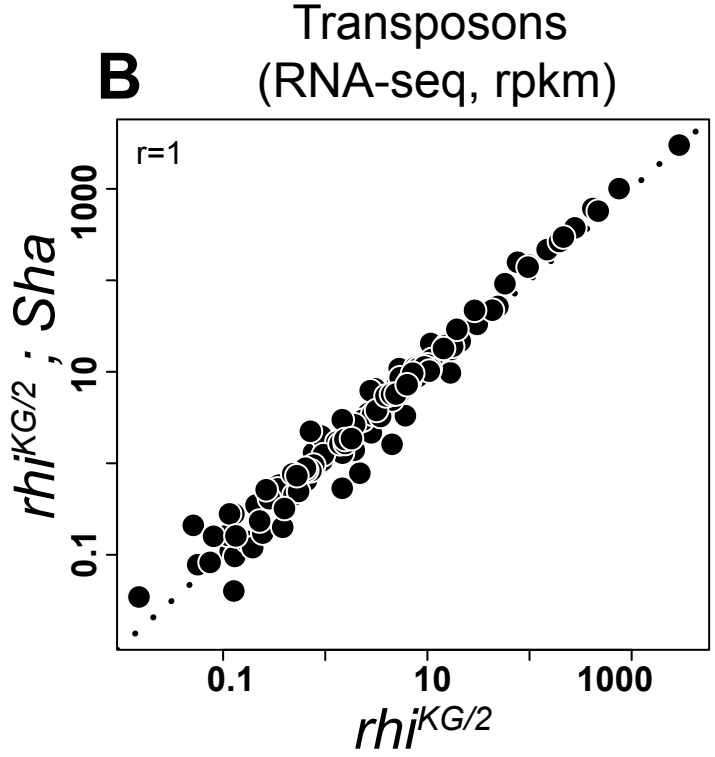
B
Transposons
(RNA-seq, rpkm)
r=1
rhiKG/2 ; Sha
rhiKG/2
0.1
10
1000

Figure S3

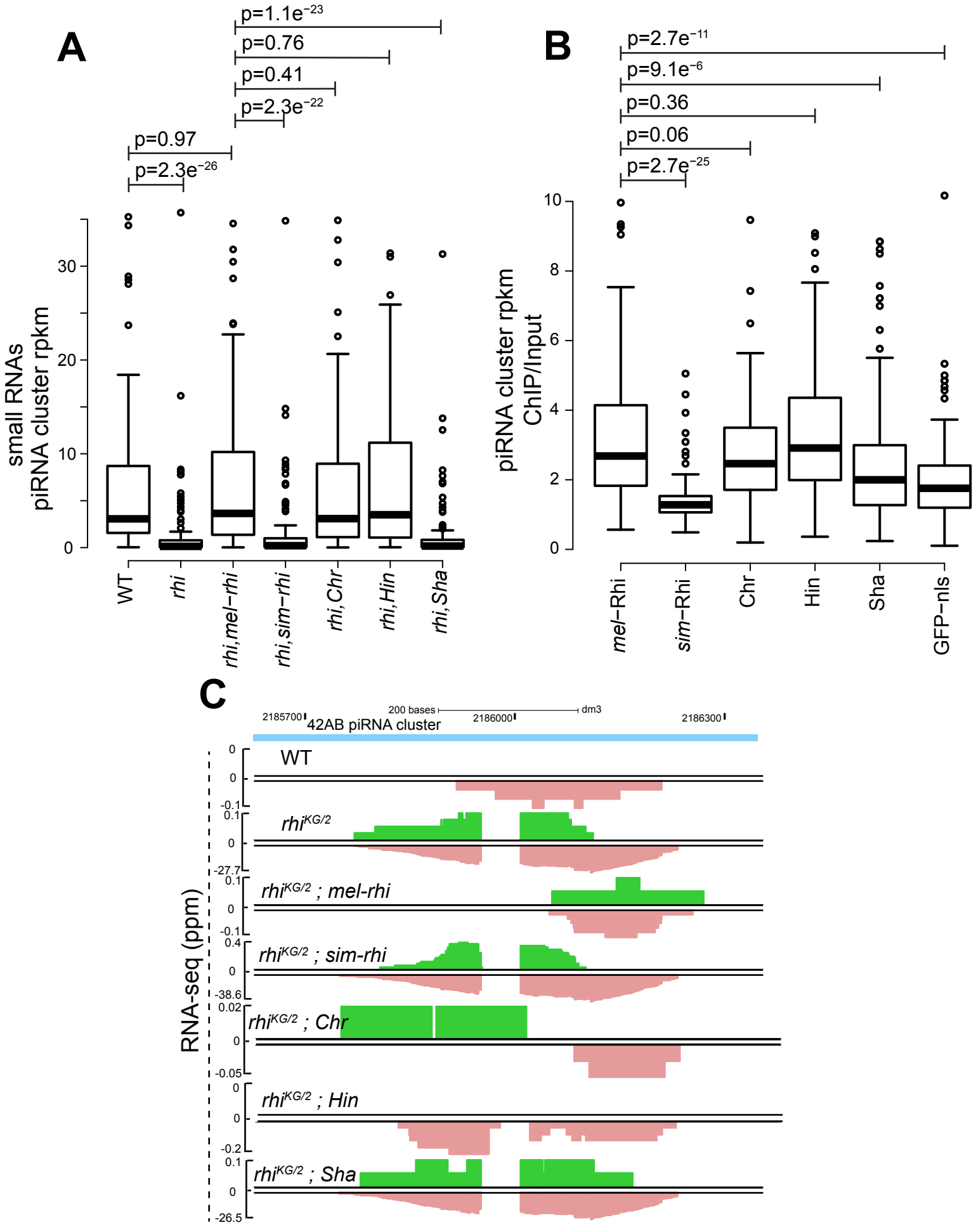
A
p=1.1e−23
p=0.76
p=0.41
p=2.3e−22
p=0.97
p=2.3e−26
small RNAs
piRNA cluster rpkm
0
10
20
30
WT
rhi
rhi,mel−rhi
rhi,sim−rhi
rhi,Chr
rhi,Hin
rhi,Sha
B
p=2.7e−11
p=9.1e−6
p=0.36
p=0.06
p=2.7e−25
piRNA cluster rpkm
ChIP/Input
0
2
4
6
8
10
mel−Rhi
sim−Rhi
Chr
Hin
Sha
GFP−nls
C
200 bases
dm3
2185700
42AB piRNA cluster
2186000
2186300
RNA-seq (ppm)
WT
rhiKG/2
rhiKG/2 ; mel-rhi
rhiKG/2 ; sim-rhi
rhiKG/2 ; Chr
rhiKG/2 ; Hin
rhiKG/2 ; Sha

Figure S4

A

nosG > GFP-Rhi

Bait protein	Spectrum counts		
	GFP	Rhi	Deadlock
mel-Rhi	60	79	24
sim-Rhi	75	73	0
GFP ctrl	187	0	0
Chromo	74	87	23
Hinge	83	89	26
Shadow	48	67	0

B

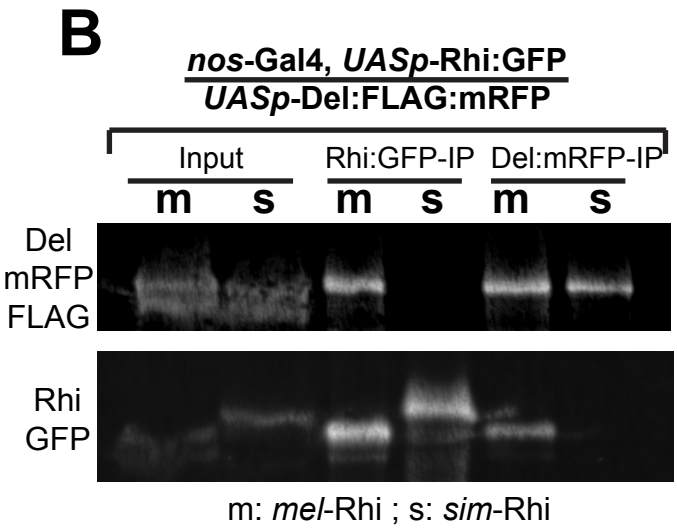

m: *mel*-Rhi ; s: *sim*-Rhi

C

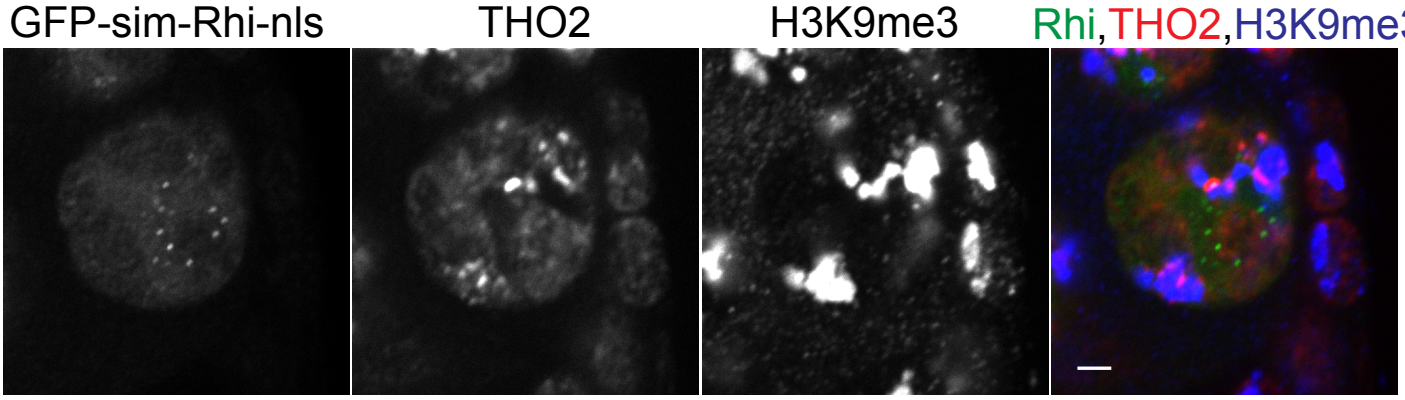

D

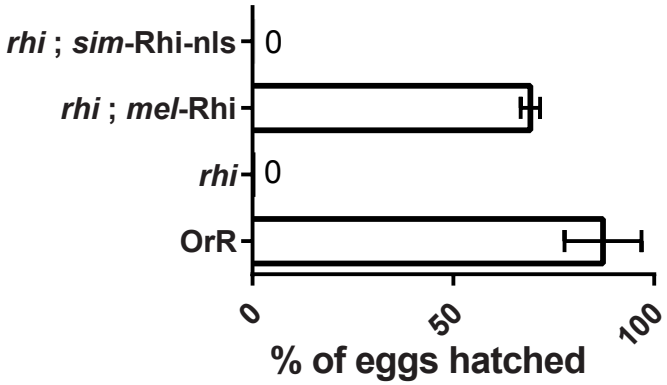

E

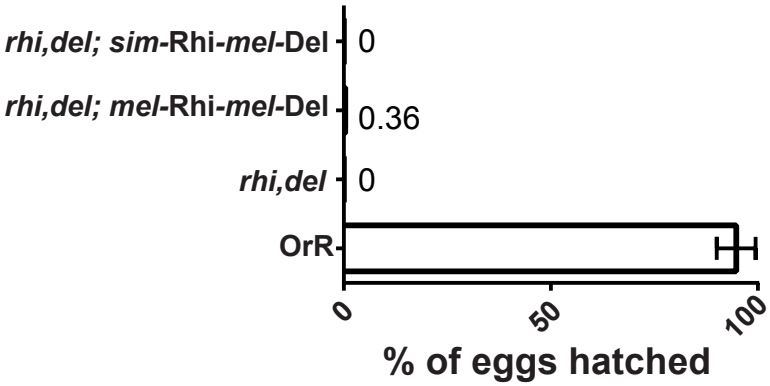

F

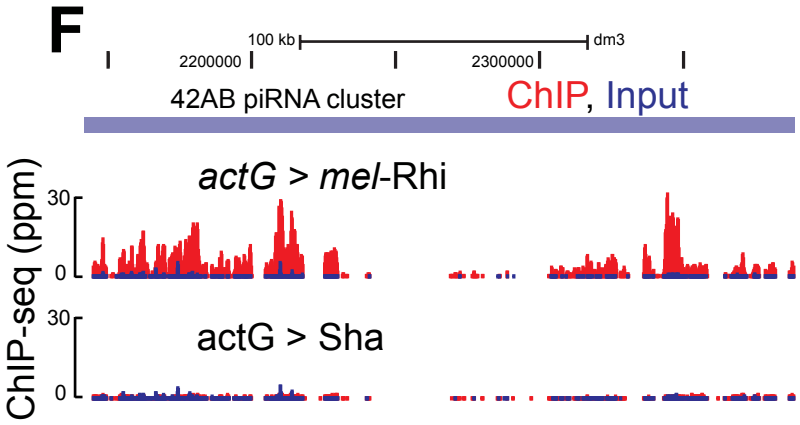

Figure S5

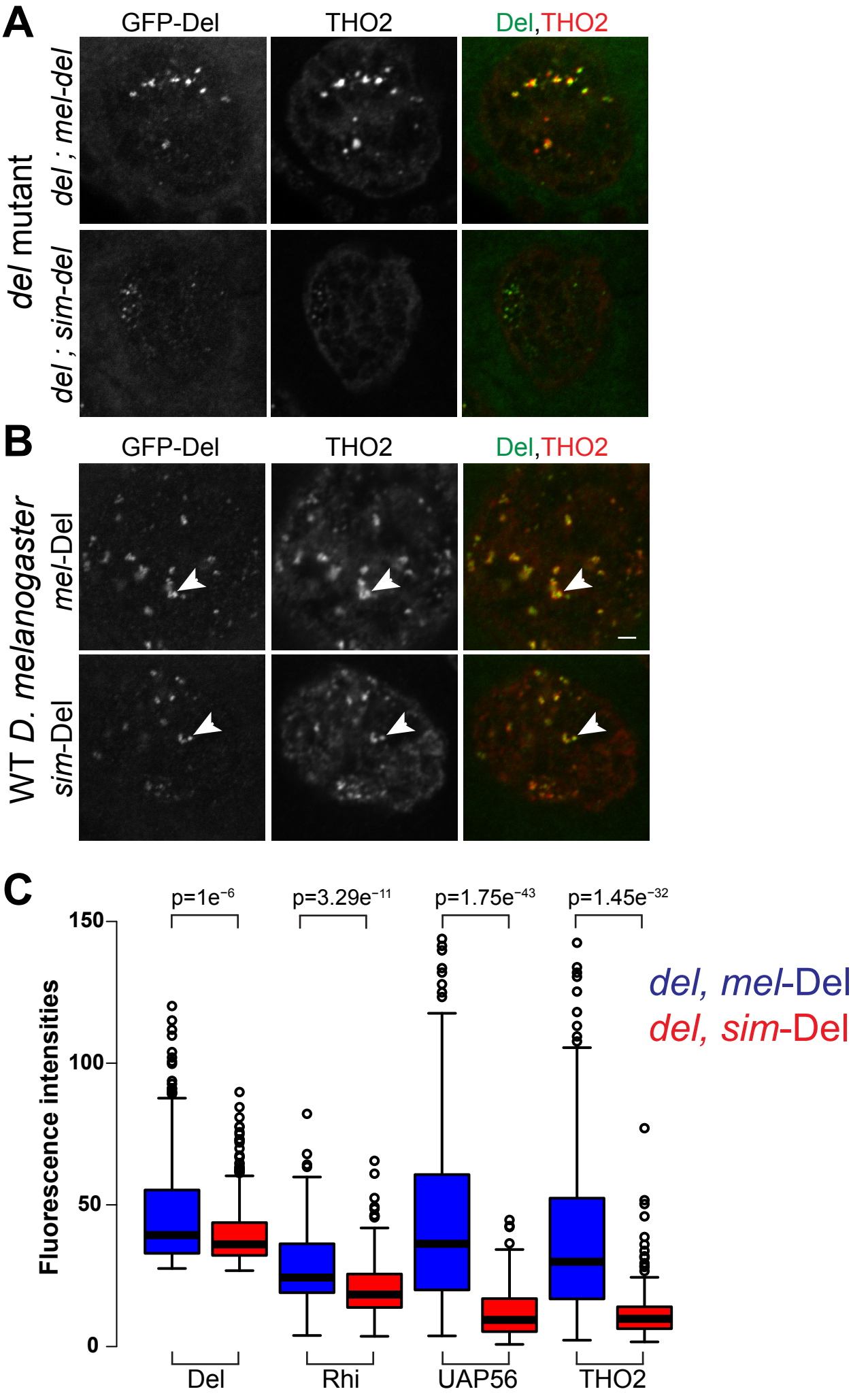
A
GFP-Del
THO2
Del,THO2
del mutant
del ; mel-del
del ; sim-del
B
GFP-Del
THO2
Del,THO2
WT D. melanogaster
mel-Del
sim-Del
C
p=1e−6
p=3.29e−11
p=1.75e−43
p=1.45e−32
150
100
50
0
Fluorescence intensities
Del
Rhi
UAP56
THO2
del, mel-Del
del, sim-Del

Figure S6

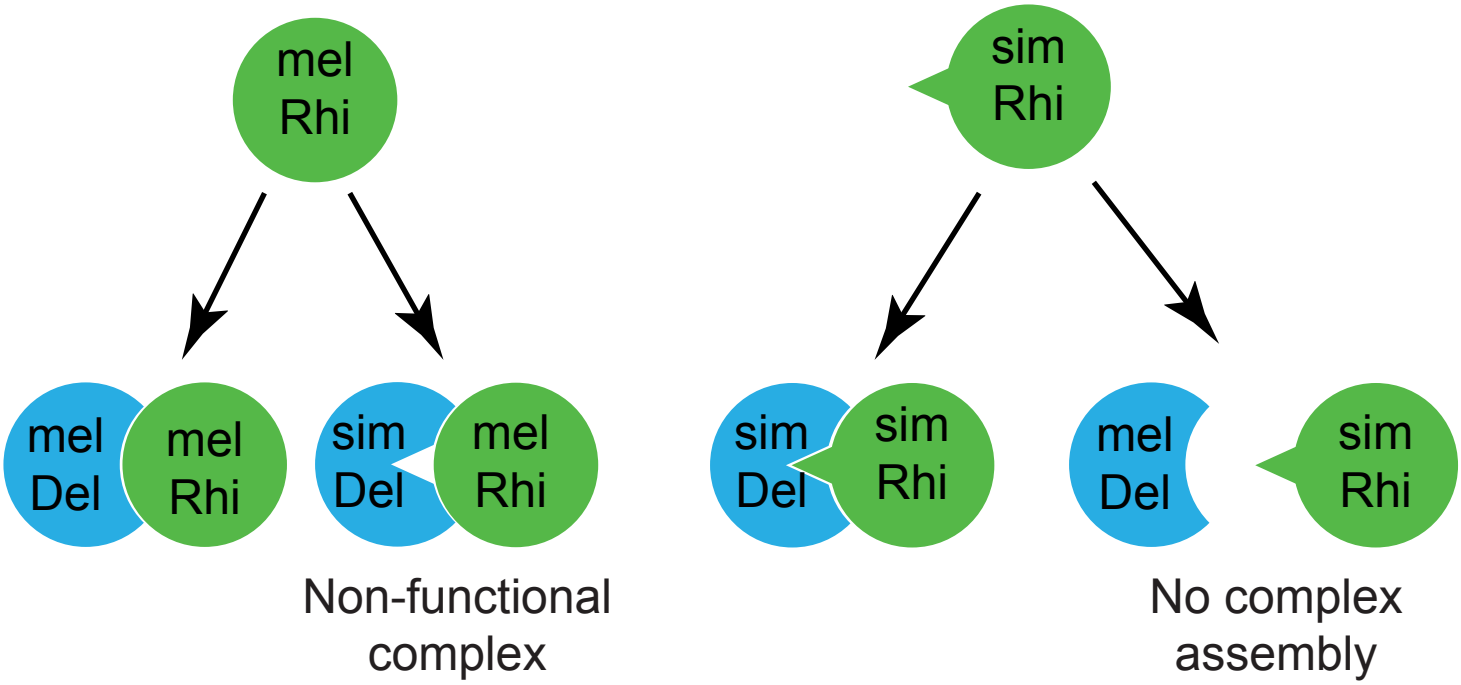
mel
Rhi
mel
Del
mel
Rhi
sim
Del
mel
Rhi
Non-functional
complex
sim
Rhi
sim
Del
sim
Rhi
mel
Del
sim
Rhi
No complex
assembly

Figure S1. Related to Figure 1. *sim-rhi* behaves like a null *rhi* allele in *melanogaster*

(A) Bar graphs showing percentages of hatched eggs from females of genotypes: OrR (WT control), *rhi* mutant, and *rhi* mutants expressing either *mel-rhi* or *sim-rhi*. The numbers in/above the bars show mean ± standard deviation of three biological replicates, with a minimum of 500 embryos scored per replicate, except for *rhi* mutants and *rhi* mutants rescued by *sim-rhi* where average of at least 30 eggs were scored.

(B) Scatterplots showing gene expression levels measured by RNA-seq in ovaries of *rhi* mutant vs. WT control. Each point represents rpkm value for a different gene. Diagonal represents x=y. p value for differences is obtained by Wilcoxon test.

(C) Scatterplots showing transposon expression levels measured by RNA-seq in ovaries of *rhi* mutant vs. *rhi* mutant expressing *sim-rhi*. Diagonal represents x=y. p value for differences is obtained by Wilcoxon test.

(D) Western blot showing *mel*-Rhi and *sim*-Rhi IPed from *melanogaster* ovaries by the GFP tag.

Figure S2. Related to Figure 2. Shadow chimera transgene behaves like a null *rhi* allele in *melanogaster*

(A) Bar graphs showing percentages of hatched eggs from females of genotypes: OrR (WT control), *rhi* mutant, and *rhi* mutants expressing either *mel-rhi* or *sim-rhi* or different chimeras. The numbers in/above the bars show mean ± standard deviation of three biological replicates, with a minimum of 500 embryos scored per replicate, except for *rhi* mutants and *rhi* mutants rescued by *sim-rhi* or Shadow chimera where average of at least 30 eggs were scored.

(B) Scatterplots showing transposon expression levels measured by RNA-seq in ovaries of *rhi* mutant vs. *rhi* mutant expressing shadow chimera. Diagonal represents x=y. p value for differences is obtained by Wilcoxon test.

Figure S3. Related to Figure 3. piRNA, ChIP-seq and RNA-seq splicing profiles for different Rhi variants

(A) Boxplot showing piRNA cluster rpkm values for small RNAs, in genotypes: WT, *rhi* mutant, and *rhi* mutants expressing either *mel-rhi* or *sim-rhi* or different chimeras. p value for differences is obtained by Wilcoxon test.

(B) Boxplot showing piRNA cluster rpkm ratios for ChIP signal to input signal, for *mel*-Rhi, *sim*-Rhi, chimeras or GFP-nls control. p value for differences is obtained by Wilcoxon test.

(C) Genome browser view of RNA-seq profiles at 42AB cluster in WT, *rhi* mutant and *rhi* mutants rescued by *mel*-Rhi, *sim*-Rhi or different chimeras. Green: Watson strand, pink: Crick strand. The scales are adjusted to prevent peak clipping.

Figure S4. Related to Figure 4. *sim*-Rhi does not bind to *mel*-Del

(A) Total spectrum counts corresponding to GFP, Rhino and Deadlock that co-precipitated with the indicated tagged proteins and GFP control. The *sim*-Rhi and shadow chimera fail to bind to *melanogaster* Del.

(B) Western blot showing that *sim*-Rhi does not bind to *mel*-Del, observed by reciprocal IP of Rhi:GFP and Del:FLAG:mRFP. m: *mel*-Rhi:GFP, s: *sim*-Rhi:GFP. Probing was done by anti-GFP (for Rhi:GFP) and anti-FLAG (for Del:FLAG:mRFP) antibodies.

(C) Localization of THO2 (piRNA cluster marker), H3K9me3 marked chromatin in the germline nuclei expressing *Act5C*-Gal4 driven GFP tagged *sim*-Rhi-nls. Color assignments for merged image shown on top. Scale bar: 2μm.

(D) Bar graphs showing percentages of hatched eggs from females of genotypes: OrR (WT control), *rhi* mutant, and *rhi* mutants expressing either *mel*-Rhi or *sim*-Rhi-nls. The numbers in/above the bars show mean ± standard deviation of three biological replicates, with a minimum of 500 embryos scored per replicate, except for *rhi* mutants and *rhi* mutants rescued by *sim*-Rhi-nls where average of at least 30 eggs were scored.

(E) Bar graphs showing percentages of hatched eggs from females of genotypes: OrR (WT control), *rhi,del* double mutant, and *rhi,del* double mutants expressing Rhi-Del fusions. The numbers in/above the bars show mean ± standard deviation of three or more biological replicates, with a minimum of 40 embryos scored per replicate.

(F) Genome browser view of ChIP-seq profiles at 42AB cluster for *act5C*-Gal4 driven GFP tagged *mel*-Rhi and shadow chimera. Both ChIP done under identical conditions, using the same anti-GFP antibody. ChIP signal in red, input signal in blue.

Figure S5. Related to Figure 6. *sim*-Del fails to recruit components of piRNA pathway

(A) Localization of THO2 in *del* mutants expressing either *mel*-Del or *sim*-Del.

(B) Localization of GFP tagged *mel*-Del and *sim*-Del in WT *melanogaster* female germline nuclei. Egg chambers were double labeled for THO2 (piRNA cluster marker). Both forms of Del co-localize to nuclear foci with THO2. Scale bar: 2μm.

(C) Boxplot showing fluorescence intensities of Del:GFP, Rhi, UAP56 and THO2 foci in del mutants expressing *mel*-Del (blue) or *sim*-Del (red).

Figure S6. Related to Figure 7. Model for directional binding incompatibility in Rhi-Del

mel-Rhi can bind to Del from both the species, but *sim*-Rhi can bind to *sim*-Del, but is incompatible with *mel*-Del. Significantly, our data indicate that the *mel*-Rhi/*sim*-Del complex is not functional.